We are IntechOpen, the world's leading publisher of Open Access books Built by scientists, for scientists

4,800
Open access books available

122,000
International authors and editors

135M
Downloads

Our authors are among the

154
Countries delivered to

TOP 1%
most cited scientists

12.2%
Contributors from top 500 universities

CLARIVATE ANALYTICS BOOK CITATION INDEX INDEXED

WEB OF SCIENCE™

Selection of our books indexed in the Book Citation Index in Web of Science™ Core Collection (BKCI)

Interested in publishing with us?
Contact book.department@intechopen.com

Numbers displayed above are based on latest data collected.
For more information visit www.intechopen.com

8

Electrospun Functional Nanofibrous Scaffolds for Tissue Engineering

Xiaochuan Yang and Hongjun Wang
Stevens Institute of Technology
United States of America

1. Abstract

Electrospinning, a high-voltage driven spinning technique, has the ability to produce nanofibers with diameter down to nanometer scale from a variety of materials. Although it is predominantly applied to polymeric materials including synthetic and natural polymers, it also allows the functionalization of nanofibers by introducing pores, and incorporating functional elements such as drugs, growth factors, or nanoparticles while electrospinning. Anisotropic nanofibrous scaffolds with spatial orientation of the electrospun nanofibers can be achieved by using the electrode configurations or the rotated collection apparatus. Three dimensional cell-rich nanofibrous constructs can be fabricated while wet electrospinning using the layer-by-layer assembly approach. Taken together, the relatively high production rate and low cost of electrospinning have drawn a great attention in materials and life sciences, especially in tissue engineering research.

2. Introduction

Tissue engineering has proven to be a promising alternative therapy to replace the lost functions of diseased tissues or organs in clinical application (Langer & Vacanti, 1993) and can provide a well defined in vitro model for drug screening or tissue related studies (Griffith & Swartz, 2006). In tissue engineering, scaffolds with high porosity and interconnectivity are normally used to provide the cells with a temporary substrate to adhere, proliferate and form new tissues. It has been recognized that the initial cell-scaffold interaction plays a critical role in regulating the later cellular phenotypic expression. Many factors, such as the surface chemistry and topography of the scaffold are involved in the cell-scaffold interaction. In this regard, more and more efforts in scaffold fabrication are now made to incorporate many instructive external cues in the scaffolds, such as immobilization of cell adhesion domains like Arginine-Glycine-Aspartic acid (RGD) on the scaffold surface or inclusion of growth factors in the scaffolds for a guided tissue formation (Lutolf & Hubbell, 2005).

In order to maintain the proper cell phenotype similar to that in the native tissues, we have proposed the biomimetic design of scaffolds to maximally recapture the major features of the native extracellular matrix (ECM) at a multiscale level, from the composition,

morphology, topography, to spatial organization. In many cases, the cells in native tissues either are embedded in ECM fibres, such as the dermal fibroblasts in skin tissue, or reside on the top of basement membrane consisting of tightly cross-linked ECM fibres with pores, such as the endothelial cells on the luminal surface of blood vessels (Abrams et al., 2000). Clearly, nanofibrous scaffolds will be preferred due to their similarity to ECM fibrils in both dimension and morphology. Indeed, the advantages of nanofibrous scaffold in promoting cell growth and maintaining the proper cell phenotype have been demonstrated in a number of studies (Woo et al., 2007; Min et al., 2004; Ji et al., 2006; Chua et al., 2005), which is considered as the synergistic result of both nanotopography and chemical signalling of the scaffolds (Patel et al., 2007; Wang et al., 2003). Several approaches are available to fabricate nanofibers including self assembly (Zhang 2003), phase separation (Woo et al., 2007; Barnes et al., 2007) and electrospinning (Formhals 1934; Telemeco et al., 2005; Matthews et al., 2002; Michel et al., 1999; Pham et al., 2006). Compared to other techniques, electrospinning represents a simple yet effective approach for preparing non-woven nano/microsized fibres.

Electrospinning, a high voltage driven spinning technique, has been widely used to produce nanofibers due to its easiness for use (Pham et al 2006). The setup of electrospinning is rather simple, composed of a high-voltage power supply, solution reservoir with the spinneret and a grounded collection surface. By far, many polymers including synthetic polymer, natural polymer, and the blend of synthetic and natural polymers have been successfully electrospun into micro/nanosize fibres (Chua et al., 2005; Matthews et al., 2002; Li et al., 2005; Yoshimoto et al., 2003; Moroni et al., 2006; Geng et al 2005). Depending on the materials used and electrospinning conditions, nonwoven fibrous meshes with microscale variation, for instance, in pore size and fibre diameter (Pham et al., 2006), have been successfully produced. However, it remains highly active to fabricate 3D multifunctional scaffolds with electrospun nanofibers to maximally match the native cell growing extracellular matrix. In particular, many in vivo tissues and organs exhibit hierarchical layered structures with distinct ECM composition and arrangement in each layer. These anisotropic properties not only offer the cells with distinct signalling information, but also provide the tissues with a unique mechanical performance to accommodate the physiological requirement. Taking as an example, three distinctive layers, i.e., ventricularis, spongiosa, and fibrosa are clearly recognized in heart valve (Schoen & Levy 1999). Densely packed collagen fibres are found in the fibrosa layer to provide the predominant strength and stiffness, and prevent excessive stretching of valve. Spongiosa, composed of loosely arranged collagen and abundant hydrophilic glycosaminoglycans (GAG), lubricates the relative movement between the ventricularis and fibrosa layers. Ventricularis is rich with elastin and shows radial aligned elastic fibres to enable the recoil and stretch of valve in response to the diastole and systole of heart. Therefore, it is highly desirable to incorporate these hierarchical features into our multiscale design of elaborate scaffolds using the electrospun nanofibers. Additionally, the spatial organization of various types of cells in the hierarchically layered tissues is often recognized, which offers the tissue with specialized function for each layer. For instance, two distinct cell layers are identified in the skin, where the epidermal layer (mainly keratinocytes) stays at the outmost region of the skin and is connected to the underneath dermal layer (mainly fibroblasts) via basement membrane. In this regard, it is also preferred for the scaffolds to help the organization of cells with a distinct and controllable spatial distribution. Electrospinning holds a great promise in

allowing the bottom-up assembly of various types of cells into layered nanofiber/cells constructs.

Synergistic regulation of cell behaviour by growth factors is critical for functional tissue formation (Frenz et al 1994; Wei et al., 2007). Supplement of soluble bioactive molecules in the culture medium can deliver the stimulation to the cells; however, it remains challenging to separately deliver the distinct stimulation to different types of cells in the same culture. In general, the inclusion of bioactive molecules directly into the scaffolds is considered as a practical solution to the aforementioned matter (Corden et al., 2000). Therefore, in the multiscale design of scaffolds to support functional tissue formation, it is critical to combine the hierarchical spatial arrangement nanofibers along with the incorporation of various bioactive molecules in the fibres.

In this chapter, we would like to present the feasibility of fabricating multifunctional nanofibrous scaffolds appropriate for engineering hierarchical tissue construct using electrospun nanofibers, which is a concise summary of the papers recently published from our laboratory (Yang et al., 2008 & 2009a and b) and non-published results. In these papers, polycaprolactone (PCL), a biodegradable and biocompatible synthetic polymer (Kweon et al., 2003; Ball et al., 2004), was used as the base material to explore all the possibilities. Bioactive nanofibers containing either collagen type I, bovine serum albumin (BSA) or fibronectin (FN) were obtained by electrospinning of the PCL mixture. Uniform distribution and bioactivity of these molecules in nanofibers were observed. The release of small molecules from nanofibers was controlled by the fibre diameter and initial loading amount. Nanofiber meshes with various topographical patterns resulted in various cellular responses. Multilayered 3D scaffolds with distinct distribution of bioactive molecules in between were successfully fabricated and demonstrated using PCL/Collagen and PCL/BSA nanofibers. More importantly, the cells of the same type or of different types could be assembled together with nanofibers to form 3D cell-rich constructs with either uniform cell distribution or distinct spatial arrangement.

3. Electrospinning and characterization

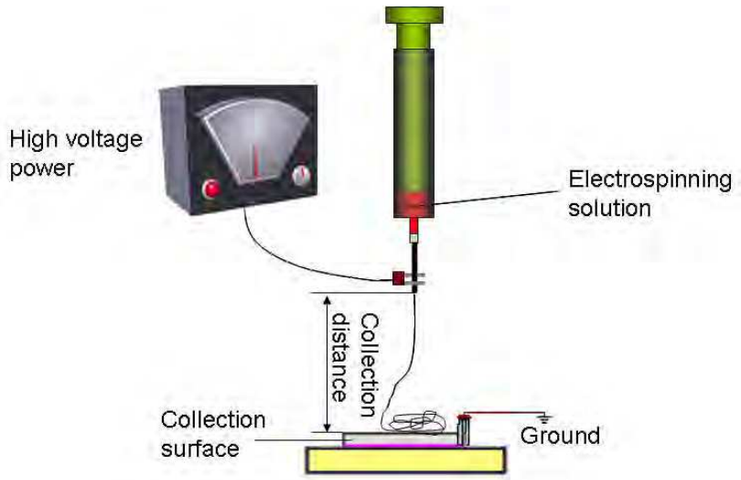

Fig. 1. Illustration of the electrospinning setup with vertical collection of fibers. Copyright 2008 Taylor & Francis Group

The typical electrospinning setup is shown in Figure 1. Using this setup, collagen-containing PCL nanofibers were successfully obtained by electrospinning the collagen-PCL blended solution (1:1 volume ratio) as reported previously (Yang et al., 2008). A common solvent of 1,1,1,3,3,3-hexafluoro isopropanol (HFIP) was used to dissolve both type I collagen and PCL solution for a well-mixed electrospinning solution in this case. The electrospinning solution was transferred to a syringe with a tip-blunt capillary (inner diameter = 0.9mm). The solution pushed out of the capillary tip by syringe pump was continuously pulled and formed the ultrathin filament under a strong electric field as shown in Figure 2A. Due to the small size of electrospun nanofibers, scanning electron microscope (SEM) was used to examine the fibres collected on Si wafer. The average diameter of electrospun fibres was determined using randomly selected SEM images. Upon optimization, the following electrospinning conditions could be used to prepare the PCL-collagen nanofibers, i.e., a flow rate between 5 μL/min and 15 μL/min, electric field strength from 0.8 kV/cm to 2.0 kV/cm and the fibre collection distance between 7 cm and 10 cm. The average diameter of PCL-collagen nanofibers was 454.5 ± 84.9 nm, and meanwhile, the surface of electrospun fibres was smooth by close examination with a SEM (Figure 2B). In addition, the pore size of the PCL/collagen nanofiber meshes that was randomly collected on Si wafer for 1 min, was noticeably below 5 μm (Figure 2A). This small interfiber distance could limit the penetration of cells to the interior of the fibrous meshes and led to the tissue formation on the peripheral surface of the meshes (Powell & Boyce, 2008).

4. Cell response to electrospun nanofibers

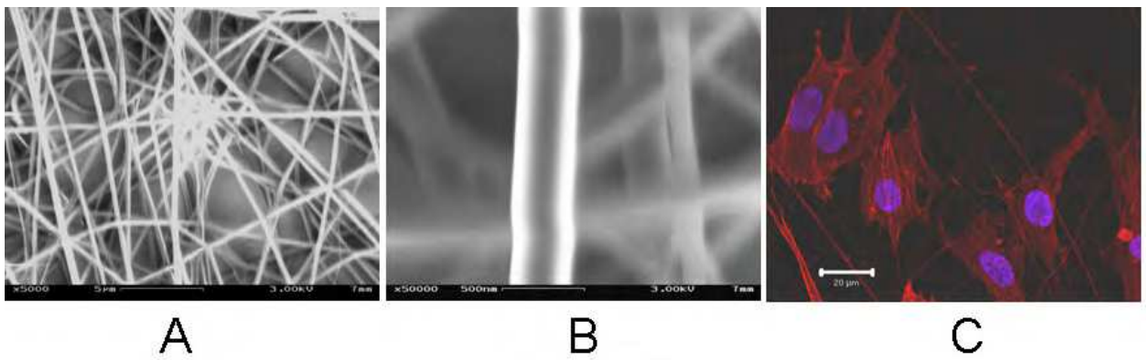

Fig. 2. Growth of neonatal human dermal fibroblasts on electrospun nanofibers. SEM image of 1:1 (w/w) PCL/collagen fibers at a low magnification (A) and high magnification (B). Confocal microscopy images of cells cultured on PCL-collagen fiber meshes (C). Cells were stained with TRITC-phalloidin for F-Actin (red) and with DAPI for cell nuclei (blue). Scale bar: 20 μm. Copyright 2008 Mary Ann Liebert Publishers

The inclusion of collagen into PCL nanofibers was considered favourable to cell attachment. In this regard, human neonatal dermal fibroblasts (HDF, passage 4-6) were used to test the cellular response to the electrospun PCL-collagen nanofibers. In this experiment, 0.5 mL of HDF cell suspension (2×10^4 cells/mL) was seeded onto the electrospun nanofiber meshes collected on glass coverslips. After 24-hour culture at 37 ^{o}C in a humidified incubator containing 5% CO_2, the culture was fixed in 4% formaldehyde/PBS fixative for 4 hours at room temperature and the cells were then stained with TRITC conjugated phalloidin

(cytoskeleton) and DAPI (cell nuclei). The stained cells were examined at ex360nm/em460nm (DAPI) and ex540nm/em570nm (TRITC) using a confocal microscope. Staining for cytoskeleton protein, F-actin, showed that human dermal fibroblast spread nicely on the surface of PCL/collagen fibrous meshes with a spindle-like morphology (Figure. 2C). In contrast, cells on PCL fibrous meshes remained limited spreading within the investigated time (data not shown), despite that prolonged culture could improve the cell stretch.

The biological superiority of the inclusion of collagen into electrospun nanofibers was demonstrated by the improvement of fibroblast adhesion and rapid spreading with spindle-like cell morphology. The selective attachment of dermal fibroblasts onto PCL-Collagen nanofibers instead of PCL nanofibers demonstrated the advantage of collagen as it can promote the cell-nanofibers interaction via cell membrane integrin receptors such as $\alpha 2\beta 1$ (Tulla et al., 2001; Nykvist et al., 2000; Orr et al,. 2006). Although pure collagen can be electrospun into nanofibers (Nykvist et al., 2000; Matthews et al., 2002) and proved favorable for cell attachment (Shih et al., 2006; Rho et al., 2006), its rapid degradation leads to mechanical instability (Wang et al., 2005). The composite PCL/collagen nanofibers are considered better to mimic the native ECM in both topology and composition and have a good with mechanical stability.

5. Functional electrospun nanofibers with the potential to incorporate drug and growth factor

It is always desirable to locally release drug or growth factors from the scaffold to the attached cells. To demonstrate the possibility of incorporating drugs in electrospun nanofibers, bovine serum albumin (BSA), a model protein for drug or growth factors, was successfully incorporated into the PCL nanofibers by electrospinning the PCL solution containing different amount of BSA (BSA:PCL =1:1, 1:60 to 1:600). The collected nanofiber meshes were cut into discs (1.3 cm in diameter, n=3) and placed in a 24-well plate with 1ml phosphate buffer solution (PBS) for release study. The well plate was incubated at 37^{o}C under gently shaking (80 RPM). Samples (10 μL) were taken from the supernatant at 1 hour intervals for the first 24 hours and 24 hour intervals afterwards in the cumulative release. In continuous release study, supernatant was replaced with fresh PBS at each harvesting time point.

Uniform distribution of BSA in the electrospun fibres was confirmed by using FITC-labelled BSA at a PCL/BSA ratio of 60:1 (Figure. 3A). A rapid release of BSA from PCL nanofibers was observed for those with 1:1 BSA/PCL ratio in the continuous release experiment. Majority of BSA (about 90%) was released within the first 3 hours in 1:1 BSA/PCL nanofibers, and the release of BSA was still detectable even after 24 hours (Figure. 3B). In the cumulative release experiment, BSA release reached its plateau at about 8 hours and remained the same for rest of the experimental time (Figure. 3B). The amount of BSA released into supernatant was proportional to the initial amount loaded into the PCL fibres (Figure. 3C). When the BSA/PCL ratio decreased down to 1:60, the peak release started at approximately 24 hour in the continuous release experiment and lasted more than 6 days (Figure. 3C).

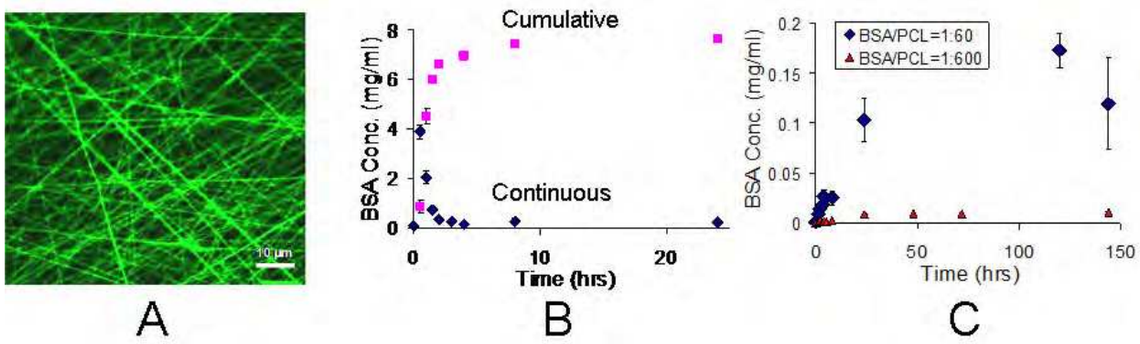

Fig. 3.The release profile of bovine serum albumin (BSA) from electrospun PCL fibers. (A) Fluorescence image of the PCL/FITC-BSA. Scale bar: 10 μm. (B) BSA release from PCL/BSA (1:1, w/w) nanofibers into PBS, measured by Lowry assay. (C) BSA released into PBS from PCL nanofibers with 1:60 or 1:600 FITC-BSA/PCL ratios, determined by fluorescent intensity. Copyright 2008 Taylor & Francis Group

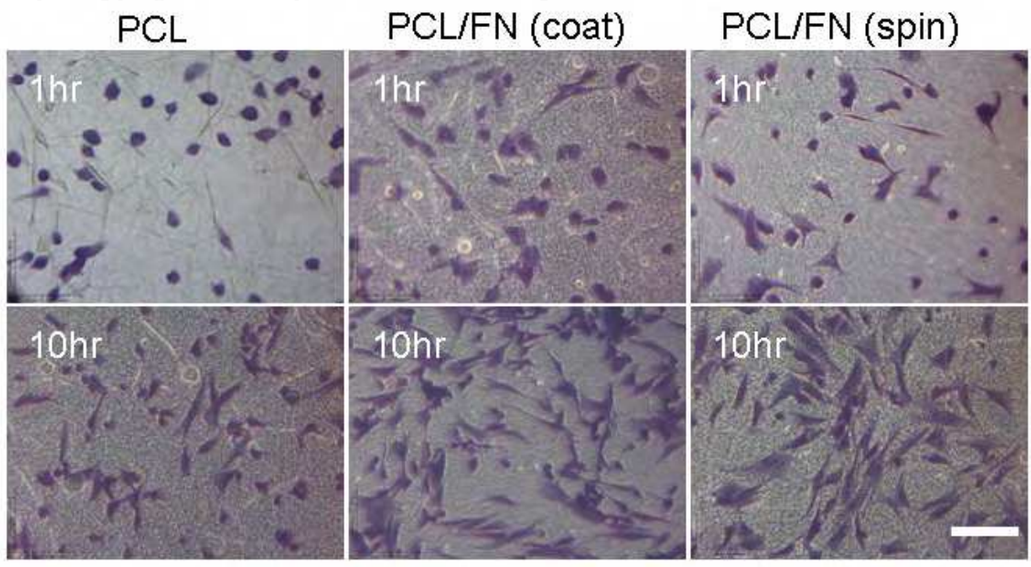

Fig. 4. Cell morphology on different nanofibrous meshes at 1 and 10 hours after cell seeding. Cells were stained with methylene blue (blue). Scale bar: 100 μm. Copyright 2008 Taylor & Francis Group

To investigate if the incorporated biomolecules into PCL fibres remain their biological activity after all the procedures for electrospinning, fibronectin (FN) (0.0125% w/w) was similarly incorporated into the electrospun PCL nanofibers as BSA. Electrospun PCL nanofibers coated with 10 μg/mL fibronectin in PBS for 1 hour were used as the positive controls and pure PCL nanofibers were used as the negative controls. Human dermal fibroblasts were seeded and cultured on all three fibrous meshes for up to 10 hours. The cell morphology on each fibrous mesh at different times was visualized by staining the fixed cells with 0.1% methylene blue. The staining results showed varying cell response to the fibres. Compared to PCL only, both PCL/FN electrospun fibres PCL/FN coated fibres showed a rapid cell spreading as early as 30 min after cell seeding (Figure 4). Majority of the cells showed spindle like morphology 10 hours after the culture on FN containing

nanofibers; in contrast, most cells still remained round shape or minimal spreading on the PCL nanofibers. To quantify the difference in cell adhesion onto different fibrous meshes, MTS assay was performed on the cells cultured on the meshes for 1 and 10 hours. Clearly, the cell adhesion onto FN containing nanofibers was significantly improved and this was observed as early as 1 hour after cell seeding (Figure 5). With the culture extended to 10 hours, more cells attached to all the investigated surfaces, but still remained a similar trend in cell adhesion, i.e., more cells were detected on the FN containing nanofibers. Necessary to mention, it seems that PCL/FN electrospun nanofibers are more favourable to cell adhesion than PCL/FN coated fibres although the mechanism is not clearly known

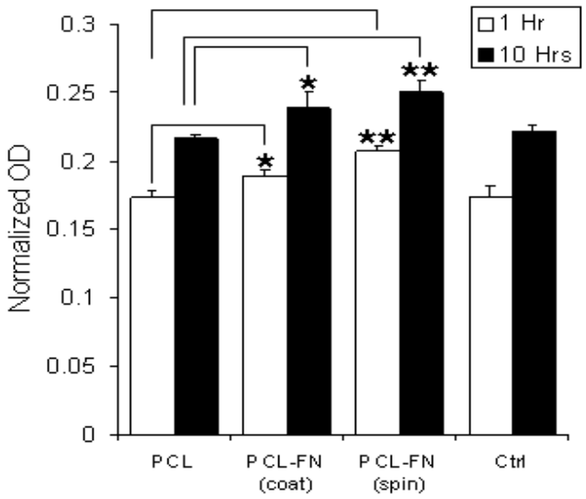

Fig. 5. Cell adhesion to different nanofiber meshes, determined by MTS assay. Representative figure out of 3 separate experiments. * $P<0.05$. ** $P<0.001$. No significant difference was observed between PCL and TCP groups. Copyright 2008 Taylor & Francis Group

It has been shown that bioactive molecules can be easily incorporated into the nanofibers by mixing them into the polymer solution. More importantly, the bioactivity remains after processing as confirmed in both collagen containing nanofibers and FN containing nanofibers. Fibroblasts similarly adhered and spread on both PCL/FN electrospun nanofibers and the PCL nanofibers coated with FN. FN enhances fibroblast adhesion and spreading mainly through the interaction with cell membrane integrins such as $\alpha5\beta1$ (Akiyama 1996). Although we did not stain for $\alpha5\beta1$, the comparable results between the two FN containing nanofibers suggest the bioactivity still remains intact after the electrospinning. This is a very important evidence for further using electrospun fibers in creation of functional scaffolds, especially for local release bioactive molecules to the attached cells. Thus, the inclusion of bioactive molecules in the nanofibers will allow us to better mimic the native ECM where numerous insoluble or soluble molecules anchor in the ECM fibers to mediate temporal cascades of cell function. Different from collagen, rapid release of BSA from the nanofibers would take place upon contact with medium. The various BSA release profiles indicate that release of bioactive molecules can be tuned to

achieve a programmable release by varying the initial drug loading, fiber diameter, spatial arrangement and fibre configuration.

6. Controlled spatial arrangement of nanofibers into various topographical patterns

In native tissues, ECM fibres with preferred orientation are often observed, leading to the anisotropic mechanical performance. The electrospinning technique allows us to control the spatial arrangement of collected nanofibers. Figure 6 (top panel) shows the PCL/collagen/BSA-FITC nanofibers collected on glass coverslips with different electric field modification. Without modifying the electric field, PCL/collagen nanofibers randomly deposited on the collecting surface. By manipulating the intensity distribution of electric field on the collecting surface, a gradient deposition of PCL/collagen nanofibers on the glass coverslip could be obtained. The aligned PCL/collagen nanofibers were achieved by applying parallel grounded metal wires on the collecting surface described previously (Ball & Shuttleworth 2004). The aligned fibres were deposited across the wires. Similarly to the aligned fibres, cross-aligned fibres with two different compositions (PCL/Collagen/FITC-BSA, and PCL/Collagen/TRITC-BSA) were obtained by using parallel wires for the first TRITC fibre and then turning the wire pair 90° for the second FITC-fibre layer.

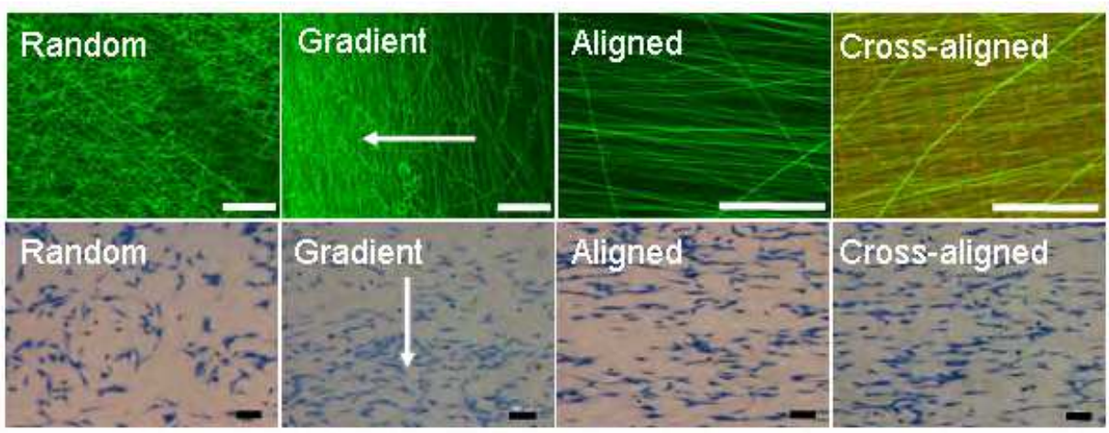

Fig. 6. Cell growth on PCL/Collagen fibrous meshes with distinctive topographical patterns. Fluorescent images of nanofibers collected on glass coverslips (Top). Green fibres labelled with FITC-BSA and red fibres labelled with TRITC-BSA. Cells cultured overnight were stained with methylene blue (blue) (Bottom). Arrow indicates the gradient direction. Scale bar: 100 μm. Copyright 2008 Taylor & Francis Group

It has been shown that the surface properties of substrates play a critical role in regulating the cell attachment. In this regard, human dermal fibroblasts were cultured on these nanofiber meshes for overnight and then stained with methylene blue. The staining results showed that cells had various distribution and spatial orientation in response to the surface configuration of collected nanofibers (Figure 6 bottom panel). On the aligned nanofibers cells oriented themselves along the direction of nanofiber alignment. However, no obvious cell orientation was observed on the randomly collected fibres. When culturing the cells on the meshes with gradient nanofiber deposition, a gradient cell distribution was

consequently achieved and higher cell number was observed in the area with high density of PCL/collagen nanofibers. Despite only a few micrometers away between green and red-fluorescent layers, the cells cultured on the cross aligned bi-layer nanofibers could only sense the nanofiber pattern with direct contact, but not the underneath one. This contact guidance inevitably includes the formation of focal adhesion composed of cytoskeletal proteins and integrin receptors (Meyle et al., 1993), and the involvement of integrin receptors can initiate the intracellular cascades to determine further cell function such as anchorage, traction for migration, differentiation, and possibly growth (Dedhar et al., 1987; Zhao et al., 2006). It has been reported that cell alignment could subsequently determine the orientation of newly deposited ECM (Manwaring et al., 2004). This implies that anisotropic new tissue formation can be controlled by designing an anisotropic scaffold. Mechanical anisotropy of aligned fibers was previously reported in several studies (Li et al., 2006; Courtey et al., 2006). A significant increase of aligned fibrous meshes in both Young's modulus (about 33 fold) and tensile modulus (about 5 fold) was measured compared to randomly collected meshes (Li et al., 2006). Ascribed to its anisotropic mechanical performance, biomechanical mimicking of soft tissues or musculoskeletal tissues using aligned fibers has multi-fold advantages and it holds tremendous promises for elaborate tissue formation with multi-functionality (see Figure 7 for the demonstration of spatial control of cell organization (non-published data)). This free control of fibre orientation can accommodate the requirements of native tissues with orientated ECM fibers changing from location to location.

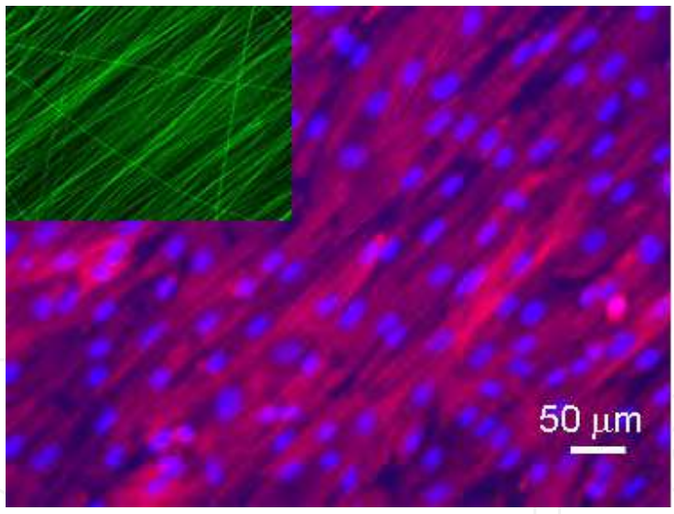

Fig. 7. Fluorescence images of the human cardiomyocytes cultured on the aligned PCL/collagen nanofibrous meshes (inset) for 24 hours. Cells were stained with TRITC-phalloidin for F-Actin (red) and with DAPI for cell nuclei (blue). Green: PCL/collagen-FITC. Scale bar: 50 μm.

7. "Layer-by-layer" 3D tissue formation

7.1 Anisotropic scaffolds with hierarchical structure

To test the capability of manipulating sequential deposition of different layers of fibres into a spatially graded scaffold, a study was performed using PCL only and PCL/Collagen containing FITC-BSA (Yang et al., 2008). The sequence was shown in Figure 8 and sequentially deposited multiple layers were directly collected on aluminium foil (substrate). The cross sections of collected scaffolds were examined under a fluorescence microscope. It was found that different nanofibers were layered into 3D meshes with an identical sequence as designed. By controlling the electrospinning time at a constant flow rate (10μl/min), the thickness of each material layer could be controlled with the designated thickness, from several micro meters to several tens of micro meters. A more confirmative result was obtained by using PCL nanofibers containing either TRITC-labelled BSA (in red color) or FITC-labelled BSA (in green color) for sequential deposition as shown in Figure 8C. The results also indicate that bioactive molecules can be incorporated into nanofibers and thereafter spatially arranged in a high order to form multifunctional scaffolds. In addition, it is intriguing to arrange cells with spatial distribution controlled by materials composition. Collagen containing nanofibers favoured the attachment of fibroblasts; therefore we hypothesized that fibroblasts would primarily attach to PCL/collagen nanofibers instead of PCL nanofibers, and lead to the controllable spatial arrangement of cells. To test this, human dermal fibroblasts were seeded and cultured in between the PCL/collagen and PCL only nanofiber layers for 24 hours. Examination of the cross-sections of cultured constructs revealed that cells only adhered to PCL/collagen nanofibers but not to the PCL ones (data not shown).

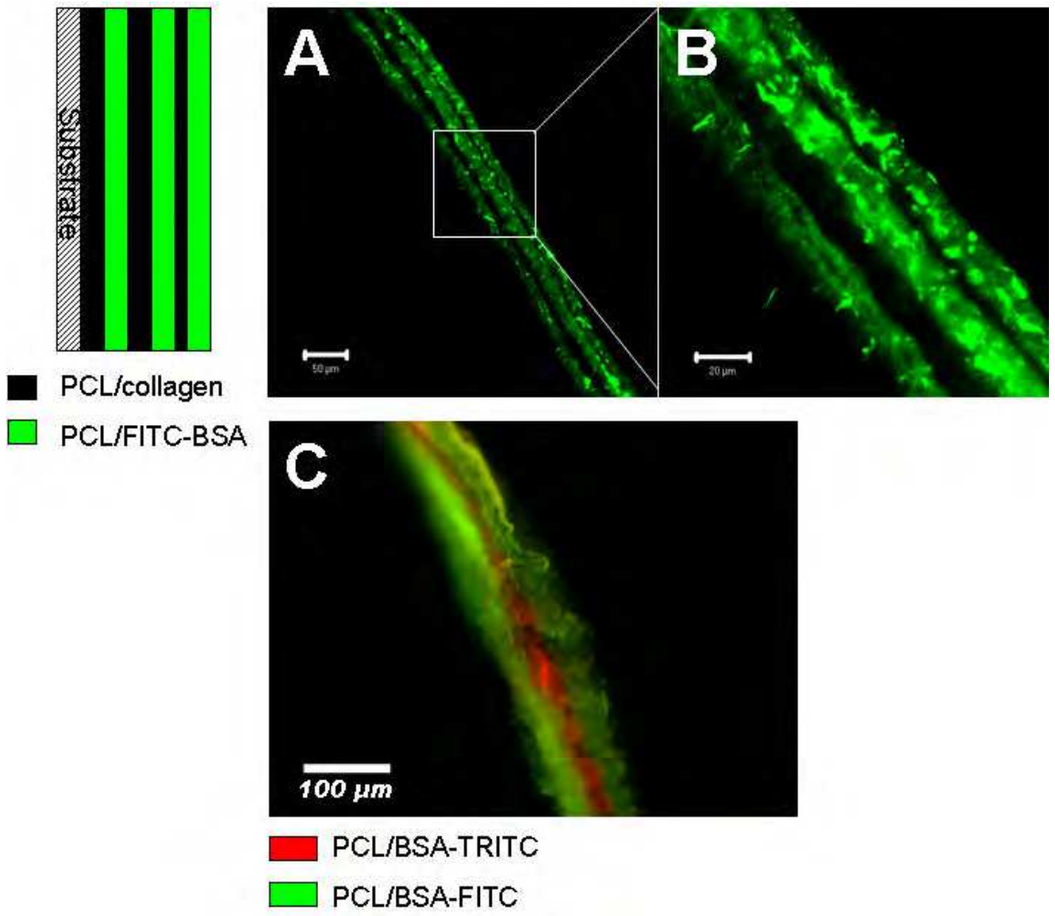

Fig. 8. Fluorescence images of transverse sections of the nanofibrous meshes. (A) and (B), multifunctional scaffolds prepared by sequentially electrospinning of solutions as designated. (B), high magnification highlighting the clear layers. (C), fluorescence images of the transverse section of a three-layer nanofibrous mesh. Red: PCL/BSA-TRITC. Green: PCL/BSA-FITC. Scale bar: (A) 50 µm; (B) 20 µm; (C) 100 µm. Copyright 2008 Mary Ann Liebert Publishers

Cells in native tissue not only experience the anisotropy from ECM fiber arrangement, but also respond to various chemistry changes from the surrounding environment. The chemical stimulation can come from the direct contact or from neighbors, and greatly depends on the spatial concentration distribution. By changing the composition of nanofibers while electrospinning, multilayered scaffolds with specified chemistry and thickness for each layer were made as designed in our study. This demonstrates the potentials to use the layer-by-layer deposition approach towards creation of cell-specific 3D microenvironment by careful selection of the nanofiber composition and the bioactive molecules incorporated into the fibres.

7.2 Layer- by- layer assembly of cell/scaffold construct

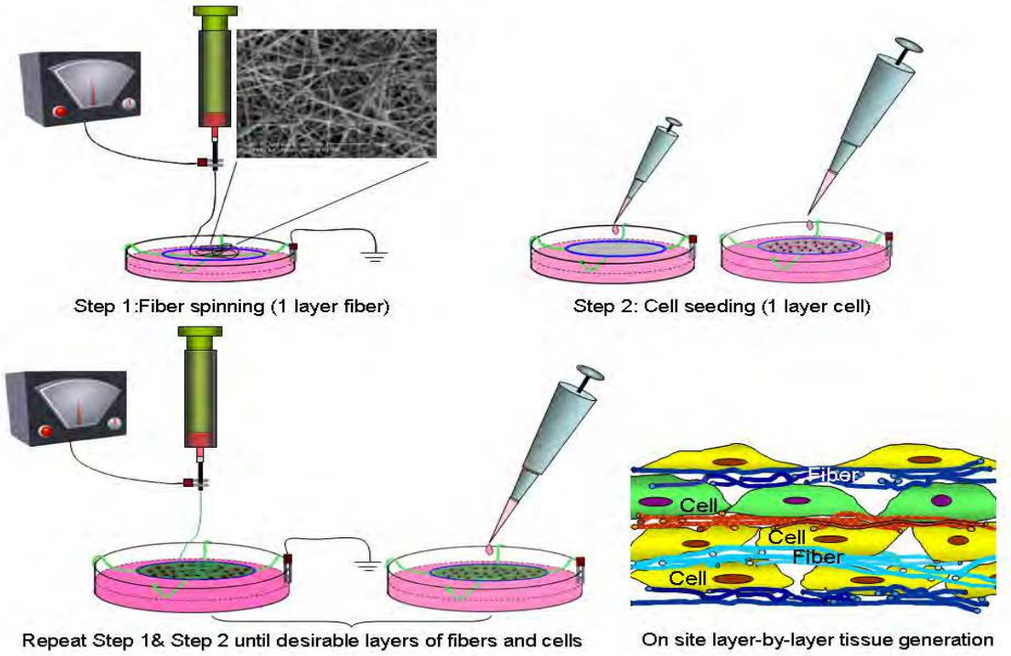

Fig. 9. A schematic illustration of the "layer-by-layer (L-b-L)" cell assembly while electrospinning. As indicated by different colours, both fibre and cell layers can be varied during the cell assembly to create a customized final 3D construct according to the design. Copyright 2008 Mary Ann Liebert Publishers

Layer-by-layer assembly of cell/nanofibers into 3D cell rich construct was recently developed in our lab (Yang et al., 2009b). While assembling the cells together with collected nanofibers to form 3D constructs as shown in Figure 9, a key step is to collect the fibre meshes on the liquid surface that is, keeping the meshes hydrated. Thus, a wet electrospinning was first developed in our lab (Yang et al., 2009b). The setup of wet electrospinning was very similar to that of conventional electrospinning (Figure 1), but with a slight modification on the fibre collection surface. In the wet electrospinning, grounded liquid was used to collect the electrospun fibres instead of using a solid metal surface. It was found the fibres deposited directly onto the liquid surface (we have tested many different liquids including the cell culture medium, phosphate buffered saline (PBS) and distilled water), and the morphology of nanofibrous meshes was very similar to those collected on the metal surface. Although the PCL/collagen fibres rapidly hydrated after depositing on the liquid surface, they remained stretched on the liquid surface without noticeable contraction. So far we have tested several other materials such as chitosan, PLGA and PCL/elastin using our wet electrospinning, and the nanofibrous meshes have been successfully obtained on the grounded water surface.

There is one potential concerns for this on site "L-b-L" cell assembly. That is, the presence of trace amount of solvent (HFIP) in the electrospun nanofibers may cause an adverse effect on the cellular function despite that most of the HFIP would evaporate during the electrospinning process. To determine the adversity to the cells, human dermal fibroblasts

were seeded and cultured on the electrospun nanofibers right after they were collected on either the medium surface or on the glass coverslip surface without further vacuum treatment as reported previously (Yoshimoto et al., 2003). The staining of cells with a dead-live kit showed negligible cell death, and most cells remained viable (Fig. 10A). Further quantification of the potential toxicity of trace HFIP was performed, in which nanofibrous meshes collected on the medium surface were left in the same culture medium and incubated for different times. The supernatants were correspondently collected and tested for cytotoxicity using MTT assay. The test result showed that no significant cytotoxicity was observed in all collected supernatants (Fig. 9B).

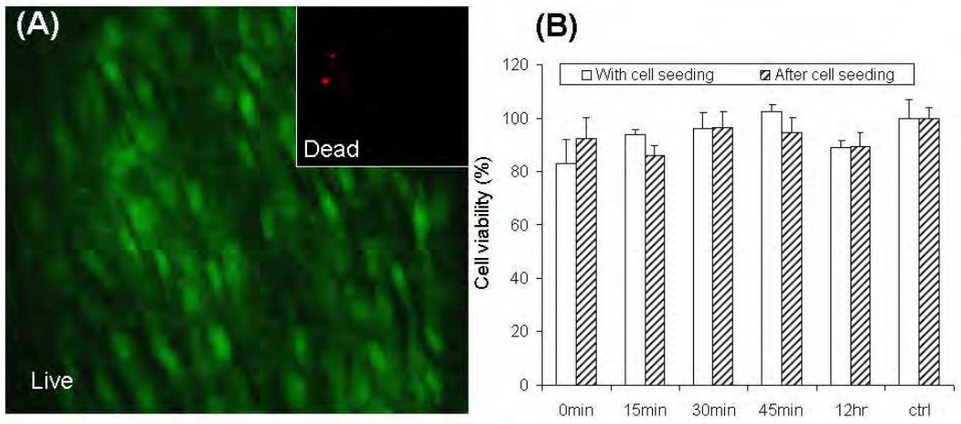

Fig. 10. Cytotoxicity of electrospun nanofibers based on a live/dead cell staining (A) and MTT assay (B). Green = live and red=dead. In MTT assay, medium samples used to extract nanofibers for different times (0 min, 15 min, 30 min, 45 min and 12h) were added to the cells along with cell seeding (white bar) or 12 hours after cell attachment (striped bar). Fresh culture medium served as controls. Data were presented as average ± SD (n = 3). Copyright 2008 Mary Ann Liebert Publishers

The feasibility of on site forming a multilayered cell structure was first evaluated by "L-b-L" assembly of human dermal fibroblasts with PCL/collagen fibres exactly following the steps as shown in Figure 9. The small inter-fibre pore size (less than 5 μm in Figure 2A) could prevent the seeded cells from escaping into the underneath medium. A total of 15 cell/fibre layers were built into a three-dimensional structure. After cultured for 2 days in Dulbecco's Modified Eagle Medium (DMEM) supplemented with 10% fetal bovine serum (FBS) and 1% Penicillin / Streptomycin, the multilayered structure was harvested and cut into thin frozen cross-sections. The staining of sections with DAPI for cell nuclei (blue) allows us to better visualize the cell spatial distribution across the full thickness of the multilayered structure. Figure 11A shows three-dimensional and yet homogeneous distribution of cells throughout the full thickness of the construct and multiple cell layers among electrospun PCL/collagen fibres could be recognized (Figure 11 A). In addition, cells in the multi-layered constructs showed elongated morphology and embedded among fibres. Figure 11B&C are the cross-sections of 7-layer fibroblast/fibre structures but with different electrospinning time for the PCL/collagen/FITC-BSA fibre layers. When the electrospinning time was 30 seconds, then around 5 μm-thick fibre layer was yielded (Figure 11B). When the electrospinning time was increased to 1 min, the thickness of nanofiber layer was correspondently increased to

around 10 μm (Figure 11C). The final shape of the built construct was defined by the metal wire loop (circular, and square loops were tested) and remained unchanged during the prolonged culture period (Figure 12).

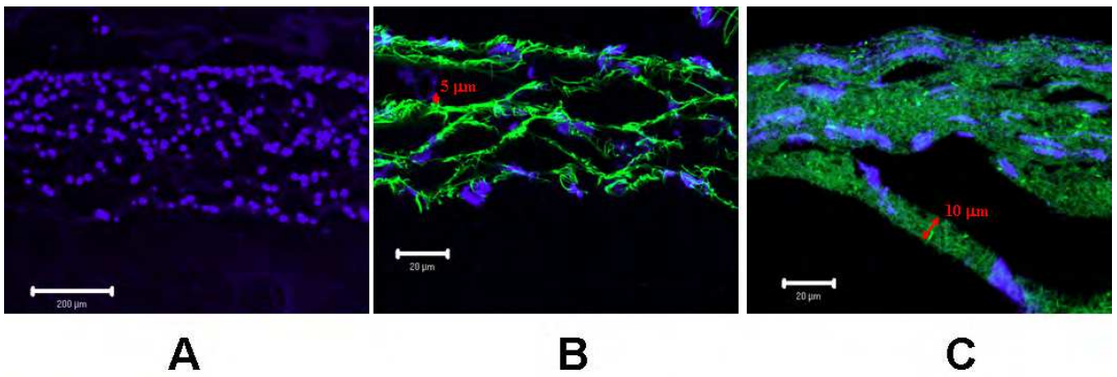

Fig. 11. Microscopic images of multilayered cell-fibre constructs: (A) Fluorescent micrograph of DAPI stained cross-sections of fibre-cell constructs cultured for 2 days. Nuclei = blue. Scale: 200 μm. (B) and (C) Confocal microscopic images of cross-sections of formed cell-fibre constructs with controlled thickness of fibre layer. Scale: 20 μm. Fibres were labelled with FITC (green) and cells were stained blue by DAPI. The images shown are representative of three separate experiments. Copyright 2008 Mary Ann Liebert Publishers

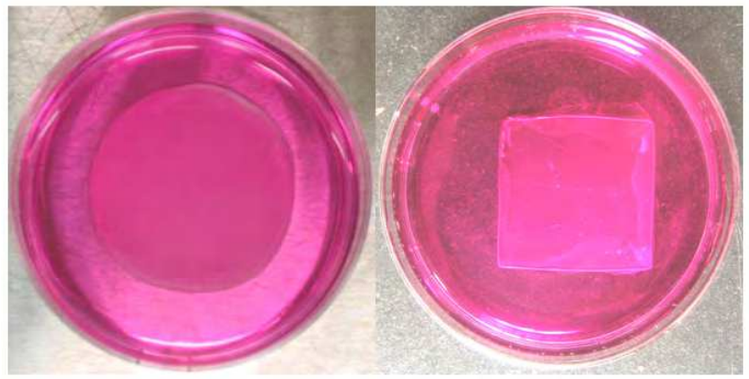

Fig. 12. Images of multilayered cell-fibre constructs cultured for 7 days on the metal wire loop with various shapes. Copyright 2008 Mary Ann Liebert Publishers

Clearly, this "L-b-L" cell assembly represents a bottom-up approach with a great degree to control the spatial distribution of cells. Most importantly, this approach provides a unique solution to the big challenge confronted with the use of electrospun nanofibrous meshes, i.e., the difficulty in penetrating the cells into the interior of the meshes.

7.3 Skin tissue formation from "L-b-L" built cell-fiber construct

As shown above, human dermal fibroblasts could be easily incorporated into the electrospun fibrous meshes along the electrospinning and form a 3D structure with uniform cell distribution. Using the same approach, we have assembled the dermal fibroblasts with PCL/collagen nanofibers into 10-layer fibroblast-PCL/collagen fibre constructs, which can be used as the dermal substitutes. The constructs were further cultured for 3 and 7 days to

study the new tissue formation. The cross sections of cultured constructs were examined under a fluorescent microscope. It was found that the cell/fibre construct became packed over a prolonged culture (Figure 13A and B). The staining of the cross-sections of the cultured constructs with hematoxylin and eosin (H & E) showed that fibroblasts evenly distributed in between the fibres without clear recognition of the layers. Meanwhile, the fibroblasts in the construct showed the elongated spindle morphology.

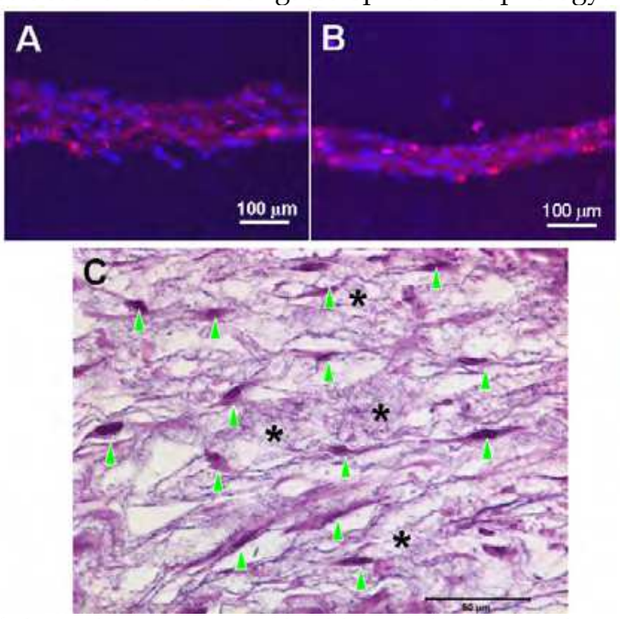

Fig. 13. Formation of dermal tissue from fibroblasts/fibre layered constructs. Fluorescent images of 10-layer fibroblasts/PCL-collagen fibre constructs (see Materials and Methods) cultured for 3 days (A) and 7 days (B). Cell nuclei stained blue, and fibres showed weak red fluorescence, though without labelling. (C) H&E stained cross-section of the construct cultured for 7 days. Arrow head indicates fibroblasts and asterisk shows fibres. Scale: 50μm. The images shown are representative of three separate experiments. Copyright 2008 Mary Ann Liebert Publishers

Using the similar layer-by-layer assembly approach, fibroblasts and keratinocytes were built with the PCL/collagen nanofibers into 3D full-thickness skin substitutes, in which 18 layers of fibroblast/fibre in the lower part were first assembled and then 2 layers of keratinocyte/fibre were assembled on the top. After culturing for three days, a bi-layer skin structure (epidermal and dermal layer) was clearly seen on the H&E stained cross sections (Figure 14A). The seeded keratinocytes remained on the surface and formed a continuous epidermal layer, and fibroblasts retained in the lower part with a uniform distribution. A tight binding between the epidermal layer and dermal layer was observed. The bi-layer structure remained the same even after culture for 7 days. With the successful assembly of two distinct types of skin cells into bi-layer skin substitutes, it is further demonstrated the flexibility of this bottom-up approach in creating multicellular and multifunctional tissues.

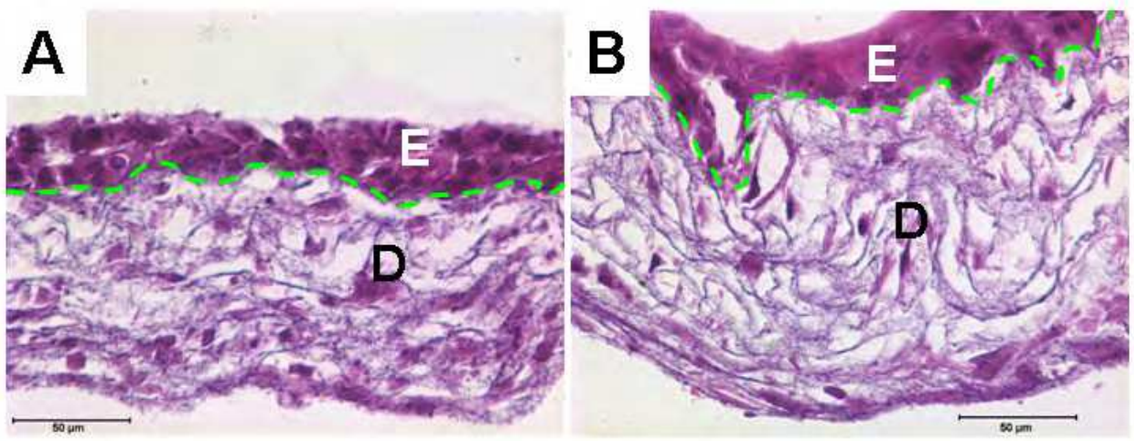

Fig. 14. H & E stained cross-sections of bi-layer skin constructs composed of epidermal (E) and dermal (D) layers and formed by culturing "L-b-L" cell assembled constructs for 3 days (A) and 7 days (B). Green broken line outlines the border between E and D. Scale: 50μm. The images shown are representative of three separate experiments. Copyright 2008 Mary Ann Liebert Publishers

7.4 Mineralized bone-like tissue formation from "L-b-L" assembled cell-fibre construct

Using this "L-b-L" bottom-up assembly approach, we have recently assembled the mouse osteoblastic cells with chitosan-containing PCL nanofibers for bone-like tissue formation (Yang et al., 2009a). The constructs composed of multilayers of chitosan/PCL nanofibers and mouse osteoblasts (MC3T3-E1 cells) were prepared and cultured for up to 28 days to determine whether chitosan-containing nanofibers could support bone-like tissue formation in a 3D setting. SEM examination of the constructs cultured for 28 days showed that the construct surface was fully covered by cells and newly formed ECM (data not shown). Examination of the cross section indicated the formation of an integral tissue across the entire thickness (Figure 15A.) and no individual nanofibers could be identified any more. The cell distribution, tissue formation and mineralization were further evaluated by histological and biochemical analyses. H & E staining of the cross-sections of the cultured constructs showed that cells uniformly distributed through the entire constructs with elongated morphology and formed an integral tissue without recognition of chitosan/PCL nanofibers (Figure 15A). Quantitative measurement of calcium content in the constructs by alizarin red staining indicated that mineralization increased with the incubation time and a significant increase in calcium deposition was observed around 21 days (data not shown). The calcium amount on Day 28 was almost 5.7 folds of that on Day 3 and only 1.6 folds of that on Day 21. Von Kossa staining of the cross-sections further revealed that mineral deposition (brownish precipitates) mainly occurred inside the cells (Figure 15B), indicating the osteogenic differentiation of MC3T3-E1.

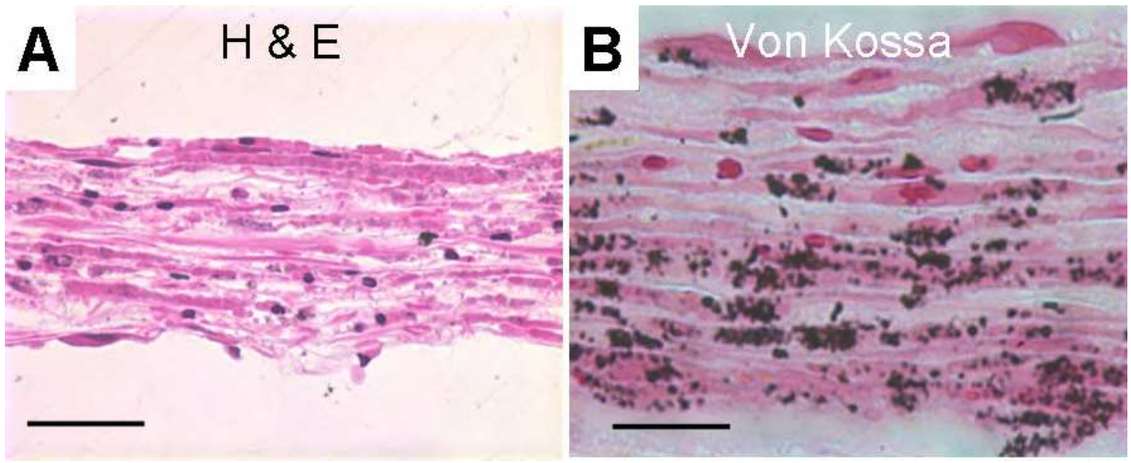

Fig. 15. (A) H&E staining of the cross-sections of 3D constructs with mouse osteoblasts (MC3T3-E1 cells) and chitosan-containing PCL nanofibers cultured for 14 days. (B) von Kossa staining of the cross-sections of 3D constructs with MC3T3-E1 cells and nanofibers cultured for 14 days. Dark brownish dots show the mineral deposition. Scale bar: A = 50μm and B = 25μm. Copyright 2009 American Chemical Society

8. Conclusions

With all the results presented in this chapter, it clearly demonstrates the feasibility of producing multiscale scaffolds with diverse functionality and tuneable distribution of bioactive molecules across the scaffold using electrospun nanofibres. This multifunctional scaffold can offer the cells with specific and customized microenvironment depending on the cell type and therefore achieve various phenotypic expressions for functional tissue formation. With the assistance of electrospun nanofibres, a new layer-by-layer bottom-up approach was developed to assemble the cells with nanofibres into 3D constructs. In this approach, cell/fibre constructs with single or multiple cell types could be assembled in an alternating manner, i.e., alternating cell layer and nanofiber layer on site of electrospinning. This new approach has multi-fold advantages, including 1) providing a uniform cell distribution throughout the nanofiber scaffold, 2) formulating the composition of each fibre layer, 3) controlling cell type for each cell layer, 4) allowing the co-culture of multiple cell types with distinct spatial arrangement. This layering process for tissue formation can provide a useful tool for engineering tissues with hierarchical structure and for in vitro studying the cell-cell or cell-materials interaction. In all, electrospinning has created a new avenue in designing biomimetic scaffolds for supporting the cell and tissue growth. With the continuous improvement of this technology, electrospinning will have many other promising applications in materials and life sciences far beyond the demonstrations presented in this chapter.

9. Acknowledgement

Majority of the results presented here were published. This publication was made possible by Grant Number R21AR056416 from NIAMS.

10. References

Abrams, G. A.; Goodman, S. L.; Nealey, P. F.; Franco, M.; Murphy, C. J., (2000) Nanoscale topography of the basement membrane underlying the corneal epithelium of the rhesus macaque. *Cell Tissue Res* 299, (1), 39-46.

Akiyama, S. K., (1996) Integrins in cell adhesion and signaling. *Hum Cell* 9, (3), 181-186.

Ball, S. G.; Shuttleworth, A. C.; Kielty, C. M., (2004) Direct cell contact influences bone marrow mesenchymal stem cell fate. *Int J Biochem Cell Biol* 36, (4), 714-727.

Barnes, C. P.; Sell, S. A.; Boland, E. D.; Simpson, D. G.; Bowlin, G. L., (2007) Nanofiber technology: Designing the next generation of tissue engineering scaffolds. *Adv Drug Deliv Rev*, 59(14),1413-33.

Chew, S. Y.; Wen, J.; Yim, E. K.; Leong, K. W., (2005) Sustained release of proteins from electrospun biodegradable fibers. *Biomacromolecules* 6, (4), 2017-2024.

Chua, K. N.; Lim, W. S.; Zhang, P.; Lu, H.; Wen, J.; Ramakrishna, S.; Leong, K. W.; Mao, H. Q., (2005) Stable immobilization of rat hepatocyte spheroids on galactosylated nanofiber scaffold. *Biomaterials* 26, (15), 2537-2547.

Corden, T. J.; Jones, I. A.; Rudd, C. D.; Christian, P.; Downes, S.; McDougall, K. E., (2000) Physical and biocompatibility properties of poly-epsilon-caprolactone produced using in situ polymerisation: a novel manufacturing technique for long-fibre composite materials. *Biomaterials* 21, (7), 713-724.

Courtney, T.; Sacks, M. S.; Stankus, J.; Guan, J.; Wagner, W. R., (2006) Design and analysis of tissue engineering scaffolds that mimic soft tissue mechanical anisotropy. *Biomaterials* 27, (19), 3631-3638.

Dedhar, S.; Ruoslahti, E.; Pierschbacher, M. D., (1987) A cell surface receptor complex for collagen type I recognizes the Arg-Gly-Asp sequence. *J Cell Biol* 104, (3), 585-593.

Formhals, A. Process and apparatus for preparing of artificial threads. *U.S. Pat*. 1975504, 1934.

Frenz, D. A.; Liu, W.; Williams, J. D.; Hatcher, V.; Galinovic-Schwartz, V.; Flanders, K. C.; Van de Water, T. R., (1994) Induction of chondrogenesis: requirement for synergistic interaction of basic fibroblast growth factor and transforming growth factor-beta. *Development* 120, (2), 415-424.

Geng, X.; Kwon, O. H.; Jang, J., (2005) Electrospinning of chitosan dissolved in concentrated acetic acid solution. *Biomaterials* 26, (27), 5427-5432.

Griffith, L. G.; Swartz, M. A., (2006) Capturing complex 3D tissue physiology in vitro. *Nat Rev Mol Cell Biol* 7, (3), 211-224.

Ji, Y.; Ghosh, K.; Shu, X. Z.; Li, B.; Sokolov, J. C.; Prestwich, G. D.; Clark, R. A.; Rafailovich, M. H., (2006) Electrospun three-dimensional hyaluronic acid nanofibrous scaffolds. *Biomaterials* 27, (20), 3782-3792.

Kweon, H.; Yoo, M. K.; Park, I. K.; Kim, T. H.; Lee, H. C.; Lee, H. S.; Oh, J. S.; Akaike, T.; Cho, C. S., (2003) A novel degradable polycaprolactone networks for tissue engineering. *Biomaterials* 24, (5), 801-808.

Langer, R.; Vacanti, J. P., (1993) Tissue engineering. *Science 260*, (5110), 920-926.

Li, D.; Ouyang, G.; McCann, J. T.; Xia, Y., (2005) Collecting electrospun nanofibers with patterned electrodes. *Nano Lett* 5, (5), 913-916.

Li, W. J.; Mauck, R. L.; Cooper, J. A.; Yuan, X.; Tuan, R. S., (2006) Engineering controllable anisotropy in electrospun biodegradable nanofibrous scaffolds for musculoskeletal tissue engineering. *J Biomech* 40, (8), 1686-1693.

Luong-Van, E.; Grondahl, L.; Chua, K. N.; Leong, K. W.; Nurcombe, V.; Cool, S. M., (2006) Controlled release of heparin from poly(epsilon-caprolactone) electrospun fibers. *Biomaterials* 27, (9), 2042-2050.

Lutolf, M. P.; Hubbell, J. A., (2005) Synthetic biomaterials as instructive extracellular microenvironments for morphogenesis in tissue engineering. *Nat Biotechnol* 23, (1), 47-55.

Manwaring, M. E.; Walsh, J. F.; Tresco, P. A., (2004) Contact guidance induced organization of extracellular matrix. *Biomaterials* 25, (17), 3631-3638.

Matthews, J. A.; Wnek, G. E.; Simpson, D. G.; Bowlin, G. L., (2002) Electrospinning of collagen nanofibers. *Biomacromolecules* 3, (2), 232-238.

Meyle, J.; Wolburg, H.; von Recum, A. F., (1993) Surface micromorphology and cellular interactions. *J Biomater Appl* 7, (4), 362-374.

Michel, M.; L'Heureux, N.; Pouliot, R.; Xu, W.; Auger, F. A.; Germain, L., (1999) Characterization of a new tissue-engineered human skin equivalent with hair. *In Vitro Cell Dev Biol Anim* 35, (6), 318-326.

Min, B. M.; Lee, G.; Kim, S. H.; Nam, Y. S.; Lee, T. S.; Park, W. H., (2004) Electrospinning of silk fibroin nanofibers and its effect on the adhesion and spreading of normal human keratinocytes and fibroblasts in vitro. *Biomaterials* 25, (7-8), 1289-1297.

Moroni, L.; Licht, R.; de Boer, J.; de Wijn, J. R.; van Blitterswijk, C. A., (2006) Fiber diameter and texture of electrospun PEOT/PBT scaffolds influence human mesenchymal stem cell proliferation and morphology, and the release of incorporated compounds. *Biomaterials* 27, (28), 4911-4922.

Orr, A. W.; Ginsberg, M. H.; Shattil, S. J.; Deckmyn, H.; Schwartz, M. A., (2006) Matrix-specific suppression of integrin activation in shear stress signaling. *Mol Biol Cell* 17, (11), 4686-4697.

Patel, S.; Kurpinski, K.; Quigley, R.; Gao, H.; Hsiao, B. S.; Poo, M. M.; Li, S., (2007) Bioactive nanofibers: synergistic effects of nanotopography and chemical signaling on cell guidance. *Nano Lett* 7, (7), 2122-2128.

Pham, Q. P.; Sharma, U.; Mikos, A. G., (2006) Electrospinning of polymeric nanofibers for tissue engineering applications: a review. *Tissue Eng* 12, (5), 1197-1211.

Pham, Q. P.; Sharma, U.; Mikos, A. G., (2006) Electrospun poly(epsilon-caprolactone) microfiber and multilayer nanofiber/microfiber scaffolds: characterization of scaffolds and measurement of cellular infiltration. *Biomacromolecules* 7, (10), 2796-2805.

Powell, H. M.; Boyce, S. T., (2008) Fiber density of electrospun gelatin scaffolds regulates morphogenesis of dermal-epidermal skin substitutes. *J Biomed Mater Res A*. 84, (4), 1078-1086

Rho, K. S.; Jeong, L.; Lee, G.; Seo, B. M.; Park, Y. J.; Hong, S. D.; Roh, S.; Cho, J. J.; Park, W. H.; Min, B. M., (2006) Electrospinning of collagen nanofibers: effects on the behavior of normal human keratinocytes and early-stage wound healing. *Biomaterials* 27, (8), 1452-1461.

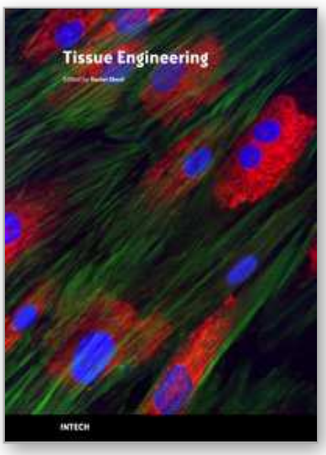

Tissue Engineering

Edited by Daniel Eberli

ISBN 978-953-307-079-7
Hard cover, 524 pages
Publisher InTech
Published online 01, March, 2010
Published in print edition March, 2010

The Tissue Engineering approach has major advantages over traditional organ transplantation and circumvents the problem of organ shortage. Tissues that closely match the patient's needs can be reconstructed from readily available biopsies and subsequently be implanted with minimal or no immunogenicity. This eventually conquers several limitations encountered in tissue transplantation approaches. This book serves as a good starting point for anyone interested in the application of Tissue Engineering. It offers a colorful mix of topics, which explain the obstacles and possible solutions for TE applications.

How to reference

In order to correctly reference this scholarly work, feel free to copy and paste the following:

Xiaochuan Yang and Hongjun Wang (2010). Electrospun Functional Nanofibrous Scaffolds for Tissue Engineering, Tissue Engineering, Daniel Eberli (Ed.), ISBN: 978-953-307-079-7, InTech, Available from: http://www.intechopen.com/books/tissue-engineering/electrospun-functional-nanofibrous-scaffolds-for-tissue-engineering

INTECH
open science | open minds

InTech Europe
University Campus STeP Ri
Slavka Krautzeka 83/A
51000 Rijeka, Croatia
Phone: +385 (51) 770 447
Fax: +385 (51) 686 166
www.intechopen.com

InTech China
Unit 405, Office Block, Hotel Equatorial Shanghai
No.65, Yan An Road (West), Shanghai, 200040, China
中国上海市延安西路65号上海国际贵都大饭店办公楼405单元
Phone: +86-21-62489820
Fax: +86-21-62489821

IntechOpen